NACA TN 2932
9249

TECH LIBRARY KAFB, NM
0066170

NATIONAL ADVISORY COMMITTEE FOR AERONAUTICS

TECHNICAL NOTE 2932

WATER-LANDING INVESTIGATION OF A FLAT-BOTTOM V-STEP MODEL AND COMPARISON WITH A THEORY INCORPORATING PLANING DATA

By Robert W. Miller

Langley Aeronautical Laboratory
Langley Field, Va.

Washington
May 1953

AFMDC
TECHNICAL LIBRARY
AFL 2811

TECH LIBRARY KAFB, NM
0066170

NATIONAL ADVISORY COMMITTEE FOR AERONAUTICS

TECHNICAL NOTE 2932

WATER-LANDING INVESTIGATION OF A FLAT-BOTTOM V-STEP MODEL AND COMPARISON WITH A THEORY INCORPORATING PLANING DATA

By Robert W. Miller

SUMMARY

A flat-bottom V-step model having a beam loading of 4.6 was subjected to fixed-trim impacts in smooth water. The tests were made at trims of 4°, 12°, and 20° and initial flight-path angles ranging from 2.7° to 20.7°. The data were obtained as time histories of draft, vertical velocity, and vertical acceleration.

The experimental results are presented as plots of nondimensional lift, draft, vertical velocity, and time against flight-path angle at contact. The trends of the results agree generally with those exhibited by models having transverse steps and high beam loadings.

Computed results determined according to the method presented in NACA TN 2814 for the calculation of hydrodynamic impact loads by the use of force-draft relationships obtained in planing are compared in time-history plots with experimental impact data. These comparisons show good agreement and indicate that this method can be applied sucessfully to the impacts of V-step models having high beam loadings.

INTRODUCTION

In the development of methods for determining the water loading during impacts of seaplanes, two general lines of approach have been used. These are (1) the development of a theory based on the assumption that during an impact the fluid flow about a seaplane hull occurs primarily in two-dimensional planes oriented normal to the keel and (2) a solution of the equations of landing impact in terms of the steady-planing properties of the seaplane. The development of the transverse-flow theory was described in references 1 and 2 and methods using the planing properties were discussed in references 3 and 4.

The present paper has two main purposes. The first purpose is to present the hydrodynamic impact data obtained from tests of a flat-bottom

V-step model having a high beam loading and, in nondimensional form, to compare the trends of these data over a range of flight-path angles and trims with similar results (presented in refs. 5 and 6) from tests of two transverse-step models. The second main purpose of this paper is to show the applicability to impacts of the flat-bottom V-step model of the method of reference 4 by using the planing properties of a geometrically similar model. The required results of planing tests with such a model are presented and are used to obtain time-history comparisons with the experimental impact results.

SYMBOLS

b	beam of model, ft
F_z	vertical hydrodynamic force, lb
g	acceleration due to gravity, 32.2 ft/sec^2
l	wetted length, ft
l'	wetted length including effect of wave rise, ft
m	mass of model, slugs
m_w	virtual mass of water, slugs
n_{i_w}	impact load factor, F_z/mg or $\ddot{z}/g$
t	time after water contact, sec
V_{pl}	steady-planing velocity, ft/sec
V	velocity, ft/sec
W	weight, lb
$\dot{x}$	horizontal velocity of model, ft/sec
z	model draft, ft
z'	model draft including wave rise, ft
$\dot{z}$	vertical velocity of model, ft/sec

$\ddot{z}$ vertical acceleration of model, ft/sec^2

γ flight-path angle, deg

ρ mass density of water, 1.938 slugs/cu ft

τ trim, deg

$\psi(\omega)$ psi-function, $\frac{1}{\omega} + \log_e \omega - 1$

$\psi^{-1}(\omega)$ inverse psi-function

Subscripts:

o at time of water contact

max maximum

Dimensionless variables:

C_Δ beam-loading coefficient, $m/\rho b^3$

C_B planing lift coefficient, $F_z \Big/ \frac{1}{2} \rho b^2 V_{pl}{}^2$

$$C_B' = \frac{C_B}{1 + \frac{m_w}{m}}$$

C_d draft coefficient, z/b

C_L impact lift coefficient, $F_z \Big/ \frac{1}{2} \rho b^2 V_o{}^2$

C_t time coefficient, $V_o t/b$

k generalized draft coefficient, $\frac{1}{2C_\Delta \sin^2\tau \cos^2\tau} \int_0^{z/b} C_B' \, d\frac{z}{b}$

ϵ impact parameter, $\tan(\gamma_o + \tau) \Big/ \tan \tau$

APPARATUS AND TEST PROCEDURE

The tests were conducted in the Langley impact basin with the test equipment described in reference 7.

The V-step model used was essentially a rigid flat plate having in the plan view a rectangular forward portion and a triangular aft portion with a 2:1 taper ratio and a C_{Δ} of 4.6. The flat-bottom transverse-step model of reference 5 and the V-bottom transverse-step model of reference 6 had beam-loading coefficients of 18.8. A view of the V-step model in testing position is presented in figure 1(a) and a sketch showing its shape and dimensions is given in figure 1(b). The model was rigidly attached to the carriage boom by means of a load-measuring dynamometer which can also be seen in figure 1(a).

The standard carriage instrumentation, described in reference 7, was used to measure time histories of the lift force and of the horizontal and vertical components of velocity and displacement. Accelerations in the vertical direction were measured by an unbonded strain-gage-type accelerometer which had a natural frequency of 105 cycles per second and was oil-damped to about 65 percent of the critical damping.

The apparatus and instrumentation used gave measurements that are believed accurate within the following limits:

Horizontal velocity, ft/sec	±0.5
Vertical velocity at contact, ft/sec	±0.2
Vertical displacement, ft	±0.03
Acceleration, g	±0.2
Time, sec	±0.005
Weight, lb	±2.0

The V-step model was tested at trims of 4°, 12°, and 20°. The initial horizontal velocity for these tests was varied from approximately 25 feet per second to 85 feet per second, and the initial vertical velocity was varied from approximately 4 feet per second to 10 feet per second. The total dropping weight of the model and drop linkage was 1,330 pounds.

Throughout each impact a simulated aerodynamic lift force equal to the total dropping weight was exerted on the model by means of the lift engine. The lift engine and the general testing procedure used are described in reference 7.

METHOD OF CALCULATION

A brief description of the equations to be used in obtaining impact loads and motions from planing results is presented. The planing results necessary for the computations and the application of the planing results to impact conditions are also discussed. The assumption is made that the model remains fixed in trim and has zero roll and yaw. A further assumption is that a wing lift force equal to the dropping weight of the model acts throughout the impact.

Basic equations.- In the analysis of reference 4, the general differential equation for the hydrodynamic force occurring during oblique water impact (fig. 2(a)) of a seaplane of arbitrary constant cross section was derived and converted into a form such that the equation was expressed in terms of the planing properties of the seaplane or model. This equation was then solved to obtain equations for the float motions which can be written as

$$-\ddot{z} = \frac{\rho b^2 V_o^2 \cos^2(\gamma_o + \tau)}{2m \cos^2\tau} C_B' \left\{\psi^{-1}\left[\psi(\epsilon) - k\right]\right\}^2 \tag{1}$$

and

$$\dot{z} = \frac{\dot{z}_o}{\epsilon - 1}\left\{\psi^{-1}\left[\psi(\epsilon) - k\right] - 1\right\} \tag{2}$$

where

$$k = \frac{1}{2C_\Delta \sin^2\tau \cos^2\tau}\int_0^{z/b} C_B' \, d\frac{z}{b}$$

These equations give the acceleration and vertical velocity of the seaplane or model in terms of the properties of the seaplane or model, the initial conditions of the impact, the generalized draft z/b, and the conventional planing coefficient C_B, as is shown subsequently.

Determination of planing coefficient.- The values of planing coefficient required for the impact computations were obtained from an analysis of planing data for a small-scale model of the V-step plate used in the impact tests. The planing results used in this analysis were in

the form of plots of wetted length, draft, and load against wetted area at various model velocities and trims.

The wetted-length and draft results were used to obtain a measure of the increase in wetted length $l' - l$ (see fig. 2(b)) caused by the wave rise generated by the motion of the model. The wetted length including the effect of wave rise, as shown in figure 3, is approximately

$$\frac{l'}{b} = 1.2\,\frac{l}{b} \qquad \left(\frac{l'}{b} < 2\right) \tag{3}$$

$$\frac{l'}{b} = \frac{l}{b} + 0.35 \qquad \left(\frac{l'}{b} > 2\right) \tag{4}$$

where

$$l = \frac{z}{\sin\tau} \qquad\qquad l' = \frac{z'}{\sin\tau}$$

The constant (0.35) increase in equation (4) is in agreement with the results obtained in reference 4 for the rectangular portion of the model and the percentage increase for the triangular portion is in accord with the scale effect of increasing similar immersed areas.

The planing coefficients computed from the load and velocity data were then plotted in figure 4 against the square of the ratio of the draft including wave rise to beam for each trim and curves were fitted to the data. Since integration of equations is simpler in this case than graphical integration in calculating the generalized draft coefficient k, the following equations were obtained from the curves in figure 4:

At a trim of 20°

$$C_B = 0.56\left(\frac{z'}{b}\right)^2 \qquad \left(\left(\frac{z'}{b}\right)^2 < 0.47\right) \tag{5a}$$

$$C_B = 0.38\left(\frac{z'}{b}\right)^2 + 0.08 \qquad \left(\left(\frac{z'}{b}\right)^2 > 0.47\right) \tag{5b}$$

At a trim of 12°

$$C_B = 0.81\left(\frac{z'}{b}\right)^2 \qquad \left(\left(\frac{z'}{b}\right)^2 < 0.17\right) \tag{6a}$$

$$C_B = 0.56\left(\frac{z'}{b}\right)^2 + 0.04 \qquad \left(\left(\frac{z'}{b}\right)^2 > 0.17\right) \tag{6b}$$

At a trim of 4°

$$C_B = 1.05\left(\frac{z'}{b}\right)^2 \tag{7}$$

Application of method.- In the case of a V-step model having a high beam loading, the virtual mass of the model is small compared with the total mass involved; therefore, in order to simplify the computations used in applying the method of reference 4, the modified planing coefficient is taken to be equal to C_B since

$$C_B' = \frac{C_B}{1 + \frac{m_w}{m}} \tag{8}$$

The impact loads and motions of the model can then be computed in the following manner: A series of values of the generalized draft z/b are chosen. By using equations (3) and (4) or the results of figure 3, the corresponding values of C_B can be obtained from figure 4 or equations (5), (6), and (7). These C_B values are then used together with the values of vertical velocity at water contact in equations (1) and (2) to obtain numerical solutions for the vertical velocity and acceleration throughout the impact. The ψ-function values required in this process are given in table I for the convenience of the reader, although values of this function are tabulated and plotted in reference 4.

The numerical solutions obtained by the use of equations (1) and (2) are in the form of "draft" histories. But since

$$t = \int_0^z \frac{dz}{\dot{z}} \tag{9}$$

integration of a plot of $1/\dot{z}$ against z will provide the necessary time function to convert the solutions so far obtained to time histories.

RESULTS AND DISCUSSION

The results of the tests are presented (1) as plots showing the variation of the nondimensional coefficients $C_{L_{max}}$, C_d, $\dot{z}/\dot{z}_o$, and C_t with flight-path angle at water contact and (2) as time-history comparisons with results computed by means of the method described in the preceding section. The trends shown in the plots of the nondimensional coefficients are compared with those for two other models of different shapes with high beam loadings. The time-history comparisons are used to demonstrate the applicability of the method to the case of V-step flat-bottom models having high beam loadings.

Experimental results.- The experimental data were obtained from the tests as time histories of draft, vertical velocity, and vertical acceleration. The values of initial conditions and the recorded data at maximum acceleration, maximum draft, and rebound are given in table II for the V-step model. The nondimensional coefficients derived from these data are affected by changes in model geometry; thus, the experimental results are valid only for models having the same shape. The results can, however, be applied to models of different size since the coefficients are general in this respect.

Figure 5 presents the variation of impact lift coefficient at the instant of maximum acceleration with flight-path angle at the instant of water contact for the V-step model. This figure shows that for the V-step model the value of impact lift coefficient increases with increasing flight-path angle but decreases slightly with increasing trim. The variation with flight-path angle is very similar to that generally observed for models having high beam loadings; however, this trend with trim is the opposite of that observed in reference 6 for a V-bottom transverse-step model. For the flat-bottom transverse-step model used in reference 5, no trend with changing trim was observed.

Figure 6 presents the draft coefficient at the instant of maximum immersion and also at the instant of maximum acceleration plotted against flight-path angle at water contact. The draft coefficient is seen to increase with increases in both flight-path angle and trim. The increase in draft coefficient with increase in flight-path angle is also observable for the two transverse-step models (refs. 5 and 6). The increase with trim is, however, observable only in the data at maximum acceleration for the flat-bottom models and not at all for the V-bottom model.

In figure 7 the ratios of the vertical velocities at the instant of maximum acceleration and at the instant of model rebound to the initial vertical velocity are plotted against flight-path angle at water contact. This figure shows that, for the V-step model at a given initial

velocity, the vertical velocity at maximum acceleration increases with increasing initial flight-path angle and decreases with increasing trim. On the other hand, again for a given initial velocity, the absolute value of vertical velocity at rebound decreases with increasing initial flight-path angle and increases with trim. These trends are similar to those exhibited by the model of reference 5 except that the results given herein for the V-step model are of nonuniform slope, whereas those of reference 5 are straight lines. No trends were observable in the velocity-ratio results for the V-bottom model of reference 6 because of the scatter of the data.

Figure 8 shows the effect of flight-path angle at water contact upon the time to reach maximum acceleration, to reach maximum draft, and for model rebound. The time coefficients at the instant of maximum acceleration and at the instant of maximum immersion decrease with increasing flight-path angle but increase with an increase in trim. For a given trim, the time coefficients for these two conditions appear to be converging as the initial flight-path angle decreases, an indication that for very small flight-path angles maximum acceleration would occur at approximately the time of maximum immersion. The time coefficient at rebound initially decreases and then increases with an increase in flight-path angle; at the lower flight-path angles, the coefficient increases with trim, whereas at the higher flight-path angles it decreases with trim.

The trends observed for the time coefficient at maximum acceleration are similar to those for the transverse-step models (refs. 5 and 6); however, for the V-bottom transverse-step model (ref. 6) the trend with trim was not well-defined. At maximum immersion the trends with trim and with flight-path angle for the V-step model were the opposite of those observed for the flat-bottom transverse-step model. The trends at the time of model rebound, for the higher flight-path angles, agree with those of the two transverse-step models; however, the results for the transverse-step models did not exhibit the reversal of trends observed at the lower flight-path angles with the V-step model.

Comparison with theory.- Time histories of the experimental draft, vertical velocity, and vertical acceleration for four of the runs listed in table II for the V-step model are compared in figure 9 with those calculated by use of the method of reference 4 for the same initial conditions. The runs chosen for the comparison are representative of the three trims used in the tests and approximately cover the range of flight-path angle covered by the tests.

In the runs shown in figures 9(a) to 9(c), the draft z appears to be overestimated by the theory throughout each impact by about 10 percent of the experimental value. The theoretical vertical accelerations $\ddot{z}$, on the other hand, closely approximate the experimental curves

except near the maximum point where the theoretical values are low. In the curves of vertical velocity $\dot{z}$ only small deviations of the theoretical data from the experimental data can be seen.

The curves for run 10 (fig. 9(d)) show even less discrepancy between the theoretical and experimental data than do the curves for the other three runs. Figure 9, therefore, indicates that the experimental results are well-represented by the results calculated by use of the method incorporating the model planing data.

The method, as presented in reference 4, has been rather extensively checked in that reference for a flat-bottom transverse-step model and the present tests provide additional evidence of the validity of the theory in general. Although these comparisons of theoretical and experimental results may not be extensive enough to give a complete validation of the theory, they should be sufficiently conclusive to permit extension of the use of the theory to flat-bottom V-step models having high beam loadings.

CONCLUSIONS

An analysis of experimental data obtained during hydrodynamic impacts of a flat-bottom V-step model having a high beam loading resulted in the following conclusions:

1. The trends with flight-path angle and trim of the plots of the nondimensional coefficients are, in general, very similar to those exhibited by transverse-step models having high beam loadings.

2. The computed motion time histories show good agreement with the experimental results, an indication that the method of NACA TN 2814 can be applied to the case of flat-bottom V-step models having high beam loadings.

Langley Aeronautical Laboratory,
National Advisory Committee for Aeronautics,
Langley Field, Va., January 16, 1953.

REFERENCES

1. Mayo, Wilbur L.: Analysis and Modification of Theory for Impact of Seaplanes on Water. NACA Rep. 810, 1945. (Supersedes NACA TN 1008.)

2. Milwitzky, Benjamin: A Generalized Theoretical and Experimental Investigation of the Motions and Hydrodynamic Loads Experienced by V-Bottom Seaplanes During Step-Landing Impacts. NACA TN 1516, 1948.

3. Steiner, Margaret F.: Analysis of Planing Data for Use in Predicting Hydrodynamic Impact Loads. NACA TN 1694, 1948.

4. Smiley, Robert F.: The Application of Planing Characteristics to the Calculation of the Water-Landing Loads and Motions of Seaplanes of Arbitrary Constant Cross Section. NACA TN 2814, 1952.

5. McArver, A. Ethelda: Water-Landing Investigation of a Model Having Heavy Beam Loadings and 0° Angle of Dead Rise. NACA TN 2330, 1951.

6. Batterson, Sidney A., and McArver, A. Ethelda: Water Landing Investigation of a Model Having a Heavy Beam Loading and a 30° Angle of Dead Rise. NACA TN 2015, 1950.

7. Batterson, Sidney A.: The NACA Impact Basin and Water Landing Tests of a Float Model at Various Velocities and Weights. NACA Rep. 795, 1944. (Supersedes NACA ACR L4H15.)

TABLE I

TABLE OF ψ-FUNCTION

$$\left[\psi(\omega) = \frac{1}{\omega} + \log_e \omega - 1\right]$$

ω	$\psi(\omega)$	ω	$\psi(\omega)$	ω	$\psi(\omega)$	ω	$\psi(\omega)$
0.01	94.3948	0.41	0.5474	0.81	0.0239	1.21	0.0171
.02	45.0880	.42	.5135	.82	.0210	1.22	.0185
.03	28.8267	.43	.4816	.83	.0185	1.23	.0200
.04	20.7811	.44	.4517	.84	.0161	1.24	.0216
.05	16.0043	.45	.4237	.85	.0140	1.25	.0231
.06	12.8533	.46	.3974	.86	.0120	1.26	.0248
.07	10.6264	.47	.3727	.87	.0101	1.27	.0264
.08	8.9742	.48	.3493	.88	.0086	1.28	.0281
.09	7.7032	.49	.3275	.89	.0071	1.29	.0298
.10	6.6974	.50	.3068	.90	.0057	1.30	.0316
.11	5.8836	.51	.2875	.91	.0046	1.31	.0334
.12	5.2130	.52	.2692	.92	.0036	1.32	.0352
.13	4.6521	.53	.2519	.93	.0027	1.33	.0371
.14	4.1768	.54	.2357	.94	.0019	1.34	.0389
.15	3.7696	.55	.2204	.95	.0013	1.35	.0408
.16	3.4174	.56	.2059	.96	.0009	1.36	.0428
.17	3.1104	.57	.1923	.97	.0004	1.37	.0447
.18	2.8408	.58	.1794	.98	.0002	1.38	.0467
.19	2.6025	.59	.1673	.99	.0000	1.39	.0487
.20	2.3906	.60	.1559	1.00	.0000	1.40	.0508
.21	2.2013	.61	.1450	1.01	.0001	1.41	.0528
.22	2.0314	.62	.1349	1.02	.0002	1.42	.0549
.23	1.8781	.63	.1253	1.03	.0004	1.43	.0570
.24	1.7296	.64	.1162	1.04	.0007	1.44	.0591
.25	1.6137	.65	.1077	1.05	.0012	1.45	.0612
.26	1.4991	.66	.0997	1.06	.0017	1.46	.0634
.27	1.3944	.67	.0920	1.07	.0022	1.47	.0655
.28	1.2984	.68	.0849	1.08	.0029	1.48	.0677
.29	1.2104	.69	.0782	1.09	.0036	1.49	.0699
.30	1.1293	.70	.0719	1.10	.0044	1.50	.0721
.31	1.0546	.71	.0660	1.11	.0053	1.51	.0744
.32	.9856	.72	.0604	1.12	.0062	1.52	.0766
.33	.9216	.73	.0552	1.13	.0072	1.53	.0789
.34	.8624	.74	.0503	1.14	.0082	1.54	.0811
.35	.8073	.75	.0456	1.15	.0093	1.55	.0834
.36	.7562	.76	.0414	1.16	.0105	1.56	.0857
.37	.7084	.77	.0373	1.17	.0117	1.57	.0880
.38	.6640	.78	.0336	1.18	.0130	1.58	.0903
.39	.6225	.79	.0301	1.19	.0143	1.59	.0927
.40	.5837	.80	.0269	1.20	.0156	1.60	.0950

NACA

TABLE I.- Concluded

TABLE OF ψ-FUNCTION

ω	$\psi(\omega)$	ω	$\psi(\omega)$	ω	$\psi(\omega)$	ω	$\psi(\omega)$
1.61	0.0973	2.01	0.1956	2.41	0.2946	2.81	0.3891
1.62	.0997	2.02	.1982	2.42	.2970	2.82	.3914
1.63	.1021	2.03	.2007	2.43	.2994	2.83	.3936
1.64	.1045	2.04	.2032	2.44	.3018	2.84	.3959
1.65	.1068	2.05	.2056	2.45	.3043	2.85	.3982
1.66	.1092	2.06	.2082	2.46	.3067	2.86	.4005
1.67	.1116	2.07	.2106	2.47	.3091	2.87	.4027
1.68	.1140	2.08	.2131	2.48	.3115	2.88	.4050
1.69	.1165	2.09	.2156	2.49	.3139	2.89	.4073
1.70	.1189	2.10	.2181	2.50	.3163	2.90	.4095
1.71	.1213	2.11	.2206	2.51	.3187	2.91	.4118
1.72	.1237	2.12	.2231	2.52	.3211	2.92	.4141
1.73	.1262	2.13	.2256	2.53	.3235	2.93	.4163
1.74	.1286	2.14	.2281	2.54	.3259	2.94	.4186
1.75	.1311	2.15	.2306	2.55	.3283	2.95	.4208
1.76	.1335	2.16	.2331	2.56	.3306	2.96	.4230
1.77	.1360	2.17	.2356	2.57	.3330	2.97	.4253
1.78	.1384	2.18	.2380	2.58	.3354	2.98	.4275
1.79	.1409	2.19	.2405	2.59	.3378	2.99	.4297
1.80	.1434	2.20	.2430	2.60	.3401	3.00	.4319
1.81	.1458	2.21	.2455	2.61	.3425	3.10	.4540
1.82	.1483	2.22	.2480	2.62	.3449	3.20	.4757
1.83	.1508	2.23	.2504	2.63	.3472	3.30	.4970
1.84	.1534	2.24	.2529	2.64	.3496	3.40	.5179
1.85	.1557	2.25	.2554	2.65	.3519	3.50	.5385
1.86	.1582	2.26	.2578	2.66	.3543	3.60	.5587
1.87	.1607	2.27	.2603	2.67	.3566	3.70	.5786
1.88	.1632	2.28	.2628	2.68	.3590	3.80	.5982
1.89	.1657	2.29	.2652	2.69	.3613	3.90	.6174
1.90	.1682	2.30	.2677	2.70	.3636	4.00	.6363
1.91	.1707	2.31	.2702	2.71	.3660	4.10	.6549
1.92	.1732	2.32	.2726	2.72	.3683	4.20	.6732
1.93	.1757	2.33	.2751	2.73	.3706	4.30	.6912
1.94	.1782	2.34	.2775	2.74	.3729	4.40	.7089
1.95	.1807	2.35	.2800	2.75	.3752	4.50	.7263
1.96	.1831	2.36	.2824	2.76	.3776	4.60	.7435
1.97	.1856	2.37	.2848	2.77	.3799	4.70	.7603
1.98	.1882	2.38	.2873	2.78	.3822	4.80	.7770
1.99	.1906	2.39	.2897	2.79	.3845	4.90	.7933
2.00	.1932	2.40	.2921	2.80	.3868	5.00	.8094

NACA

TABLE II

DATA FROM TESTS OF A FLAT-BOTTOM V-STEP MODEL

[W = 1330 pounds; C_Δ = 4.6]

Run	τ, deg	At contact				At $(n_{i_w})_{max}$				At z_{max}		At rebound	
		V_o, fps	$\dot{x}_o$, fps	$\dot{z}_o$, fps	γ_o, deg	t, sec	n_{i_w}	z, ft	$\dot{z}$, fps	t, sec	z, ft	t, sec	$\dot{z}$, fps
1	4	75.6	75.4	5.8	4.4	0.053	2.4	0.28	4.8	0.138	0.41	0.389	-2.2
2		73.1	72.7	7.9	6.2	.043	3.3	.31	6.8	.130	.52	.430	-2.4
3		60.2	59.5	8.9	8.5	.040	3.8	.31	7.9	.145	.62	.585	-2.2
4	12	84.8	84.8	4.1	2.7	.140	1.3	.41	1.8	.170	.42	.377	-2.7
5		77.2	76.9	6.1	4.6	.124	2.1	.56	2.8	.149	.59	.355	-3.8
6		74.3	73.8	8.1	6.4	.102	3.1	.65	4.1	.139	.71	.349	-4.5
7		54.5	53.8	8.9	9.4	.095	2.7	.70	5.9	.170	.86	.462	-3.9
8		48.0	47.1	9.4	11.3	.089	2.4	.74	6.8	.174	.95	.544	-3.6
9		38.7	37.5	9.6	14.3	.093	2.2	.77	7.0	.210	1.08	.725	-2.6
10	20	83.8	83.7	4.5	3.0	.174	1.3	.54	1.4	.189	.54	.420	-3.3
11		73.2	72.8	7.7	6.1	.147	2.9	.84	2.6	.172	.84	.380	-5.7
12		47.3	46.2	10.0	12.2	.129	2.5	1.06	6.1	.203	1.20	.535	-5.0
13		35.9	34.5	9.9	16.0	.140	1.9	1.12	6.4	.270	1.39	.716	-3.4
14		25.9	24.3	9.2	20.7	.150	1.4	1.14	6.7	.330	1.60	1.170	-1.8

(a) Photograph of model mounted for testing.

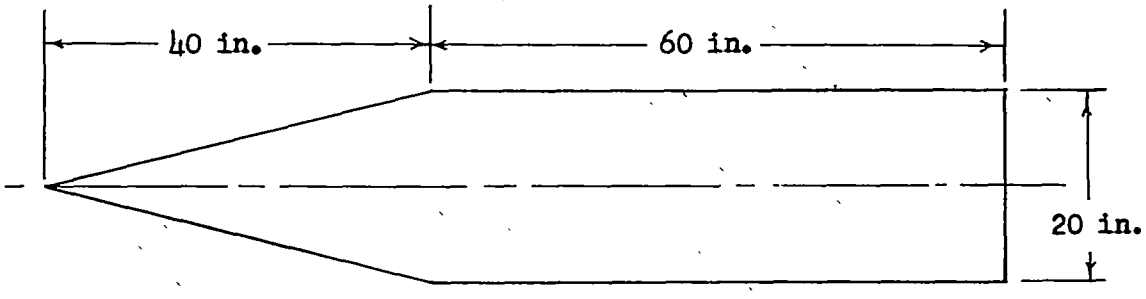

(b) Sketch of model showing dimensions.

Figure 1.- Flat-bottom V-step model having a heavy beam loading tested in Langley impact basin.

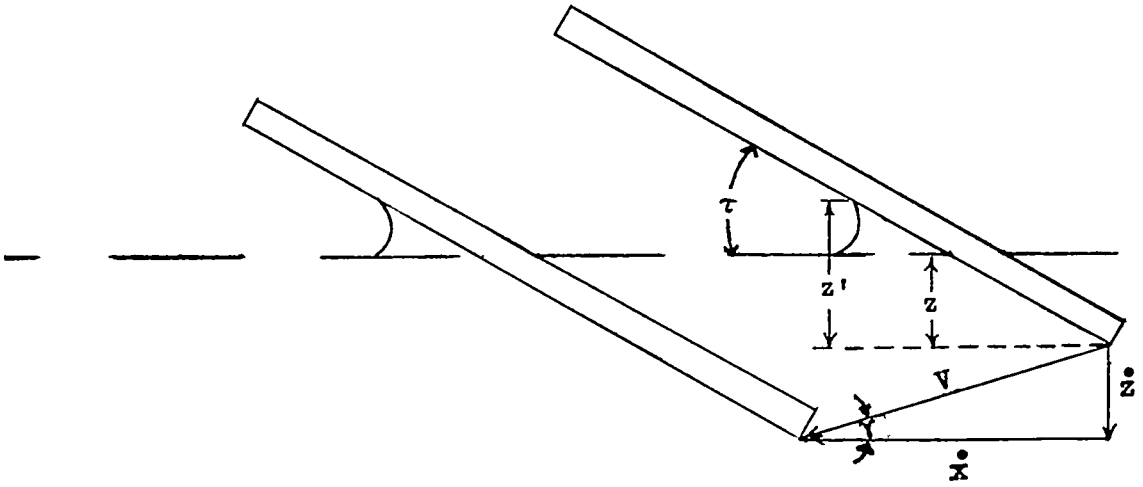

(a) Impact.

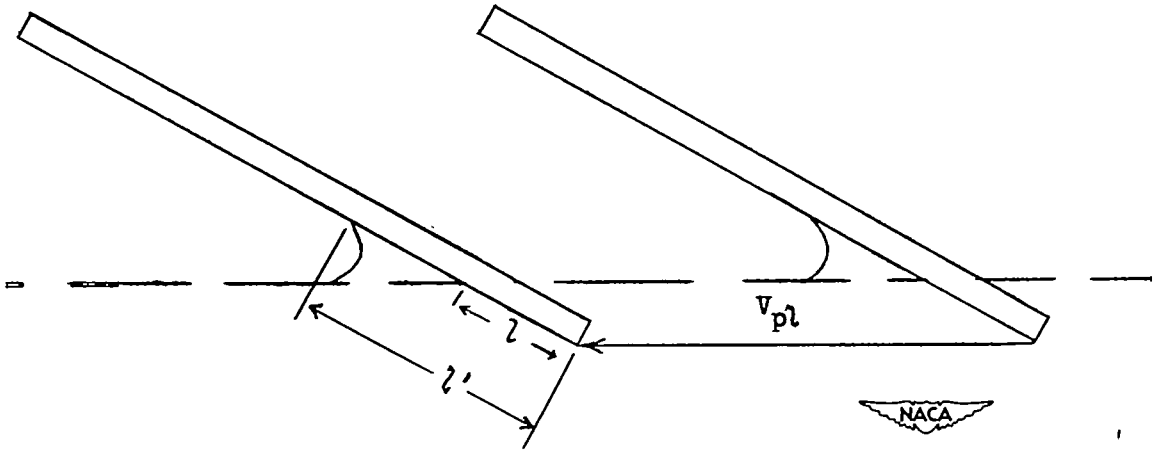

(b) Planing.

Figure 2.- Geometrical relations.

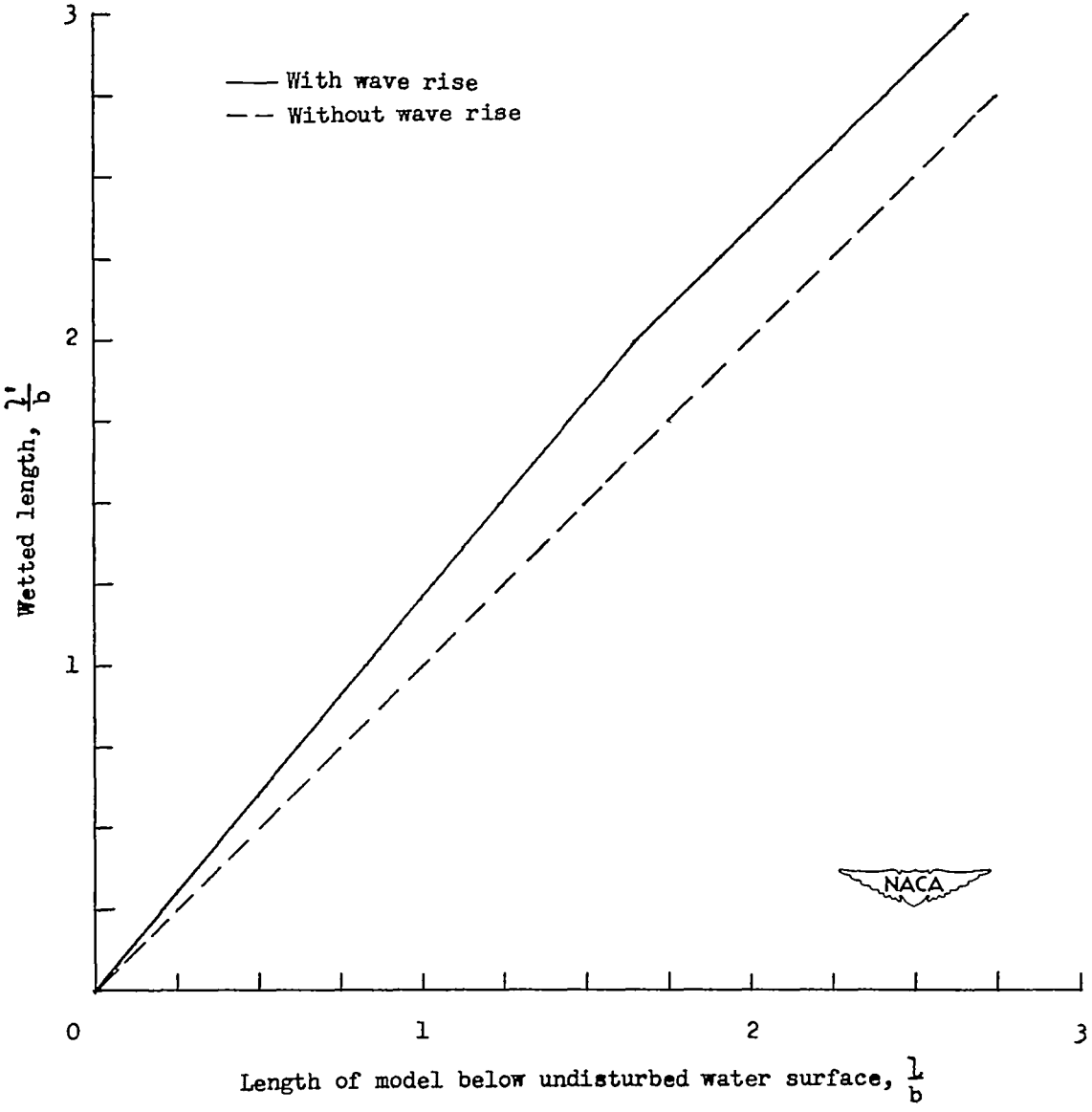

Figure 3.- Increase of wetted length due to water rise.

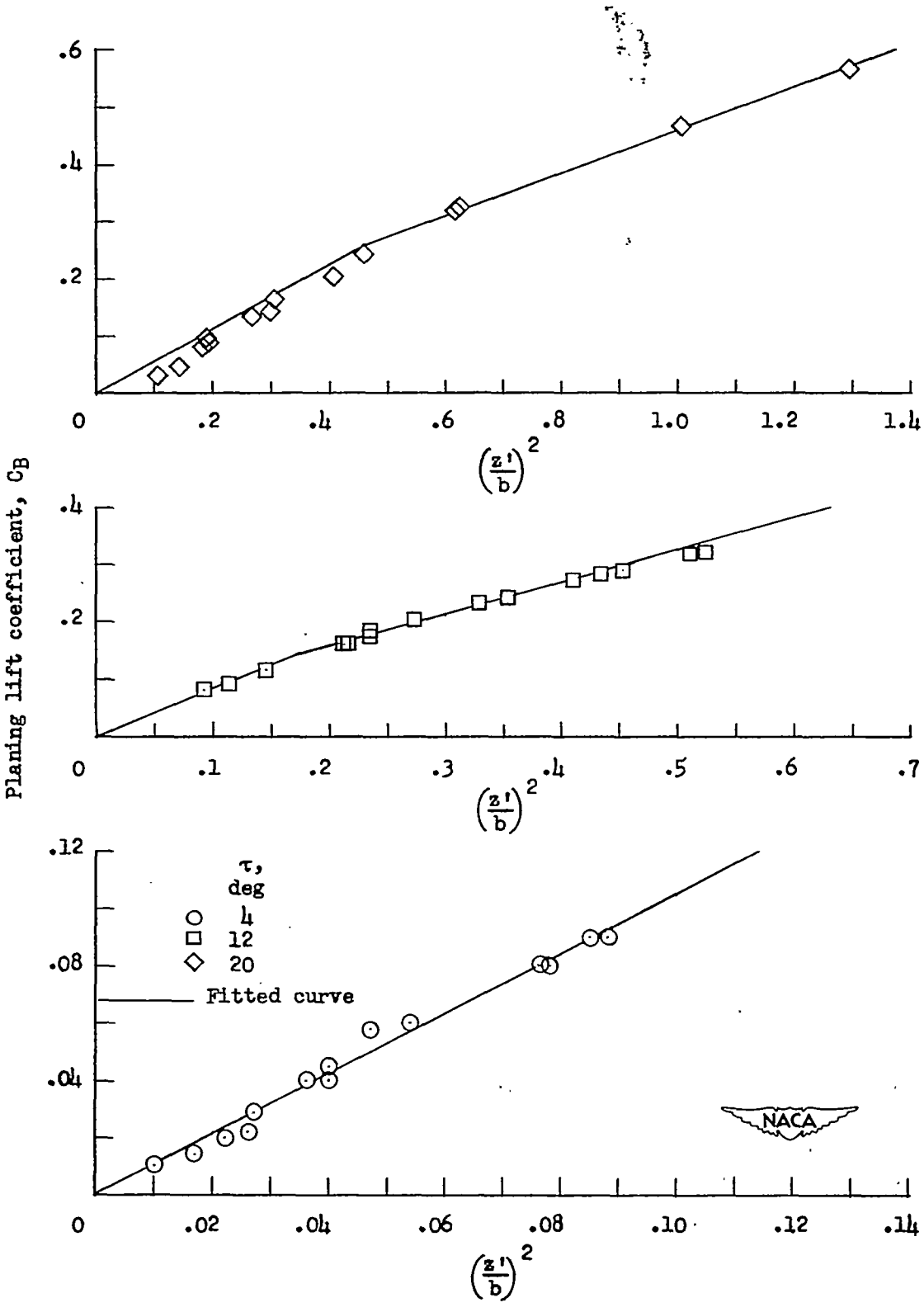

Figure 4.- Variation of planing lift coefficient with draft in beams.

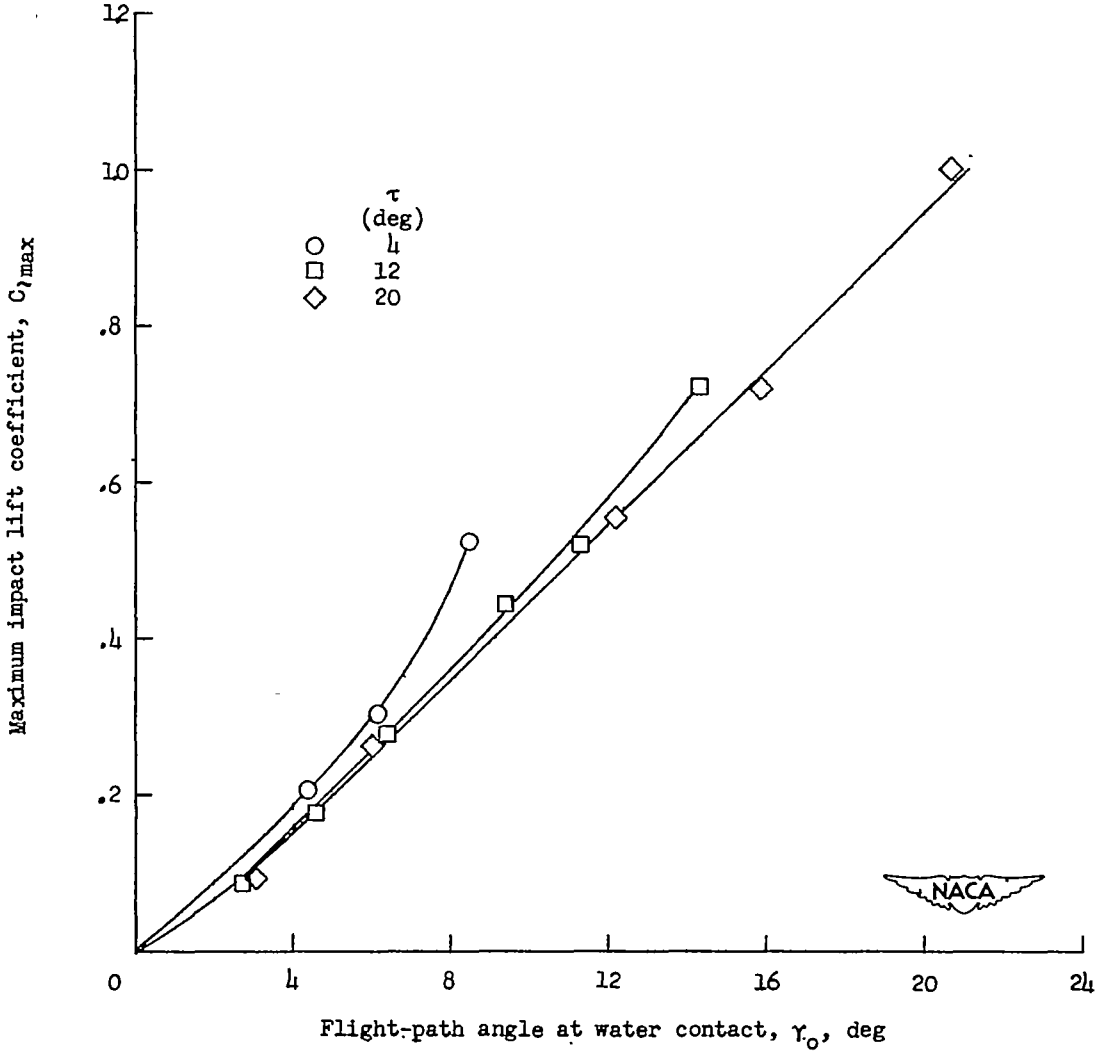

Figure 5.- Variation of impact lift coefficient at instant of maximum acceleration with flight-path angle at water contact.

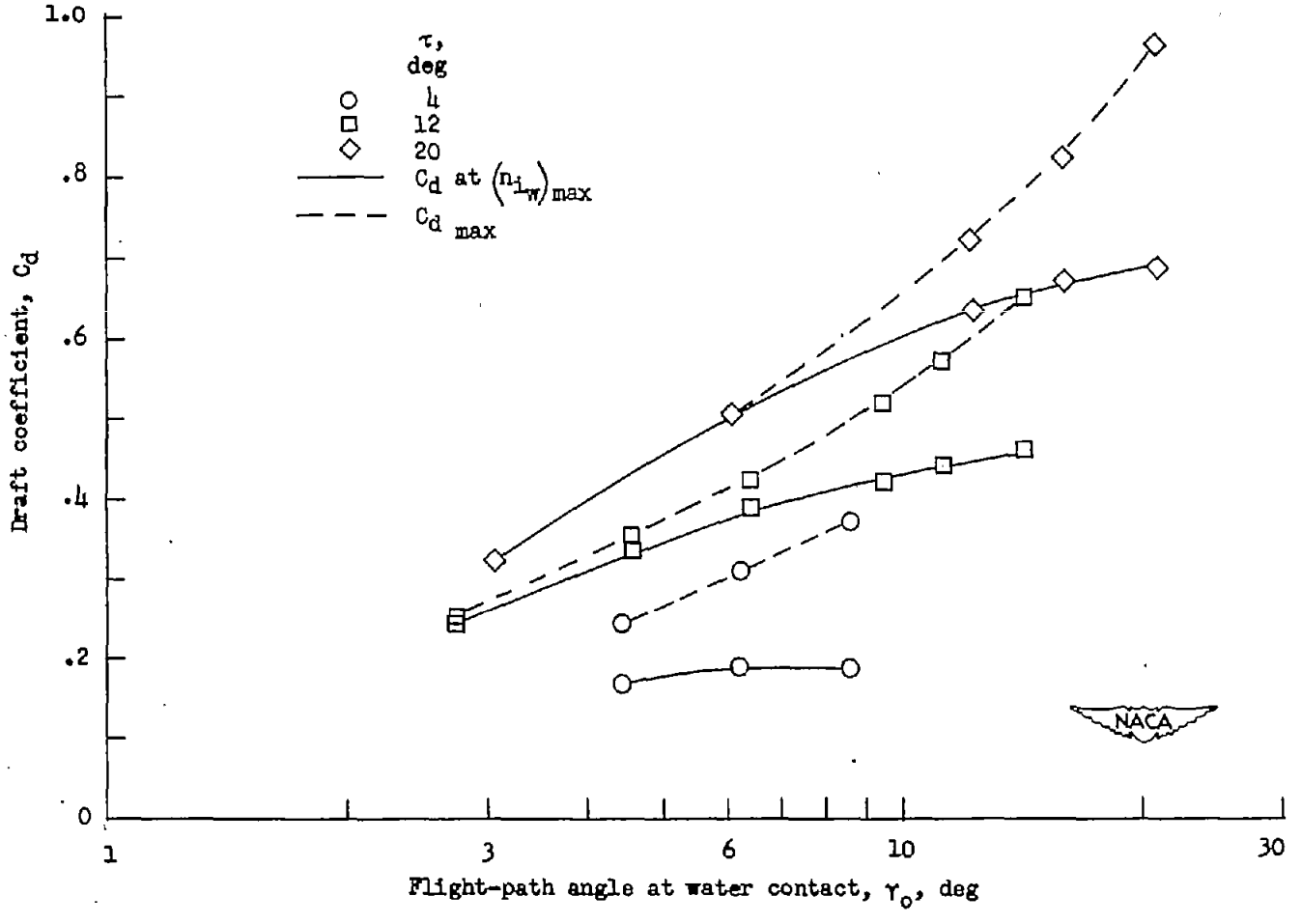

Figure 6.- Variation of draft coefficient with flight-path angle at water contact for the V-step model.

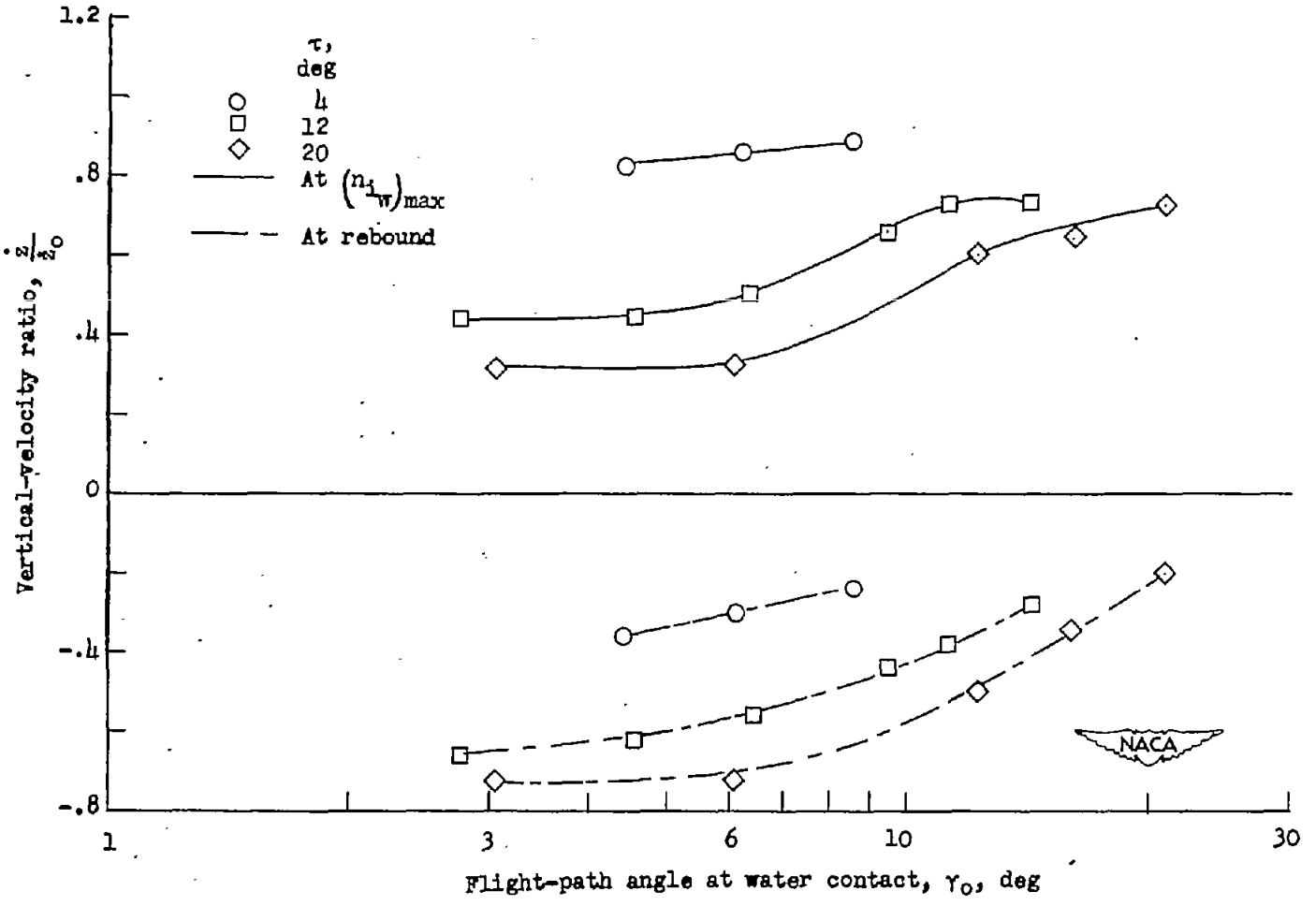

Figure 7.- Variation of vertical-velocity ratio with flight-path angle at water contact for the V-step model.

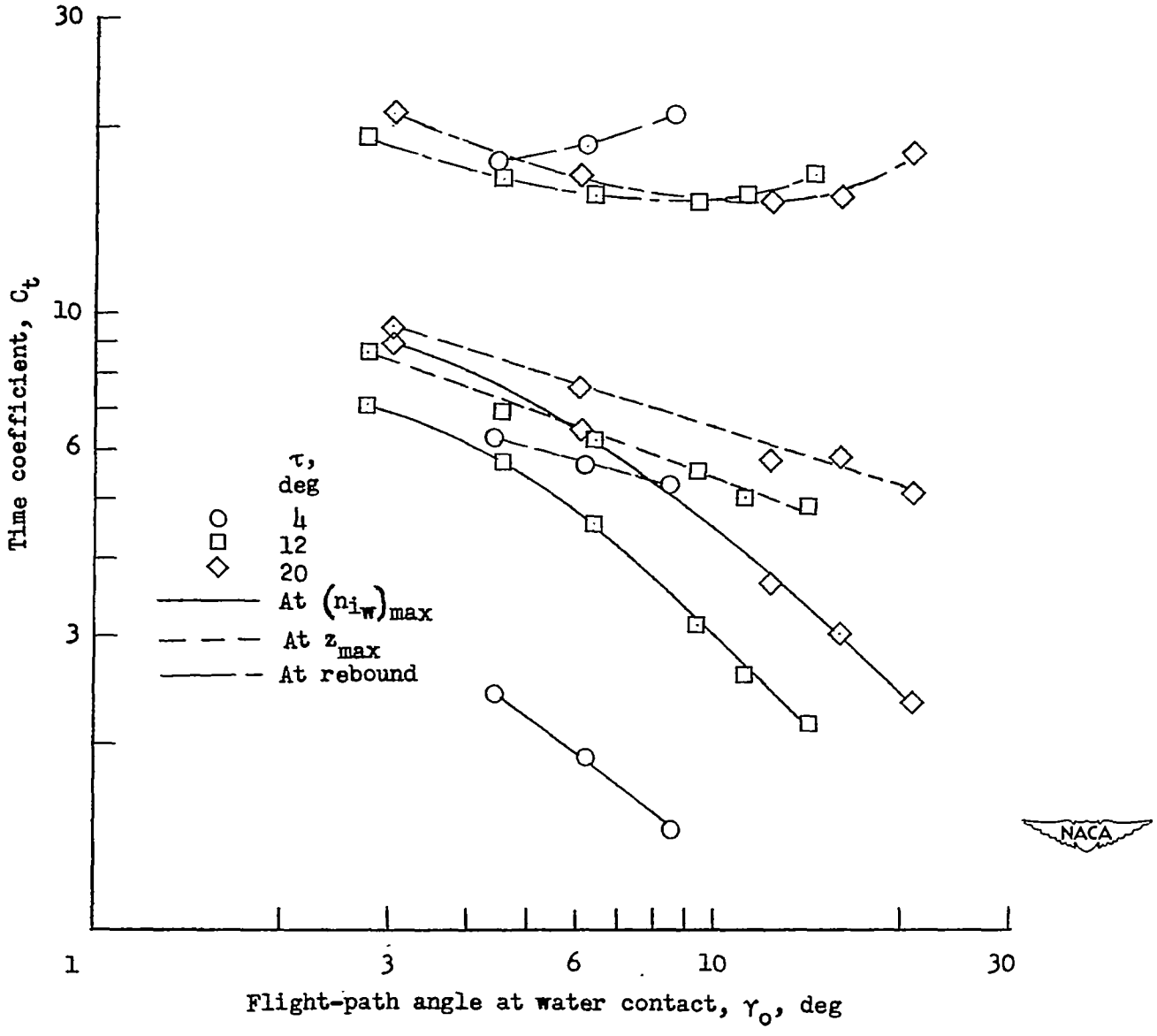

Figure 8.- Variation of time coefficient with flight-path angle at water contact for the V-step model.

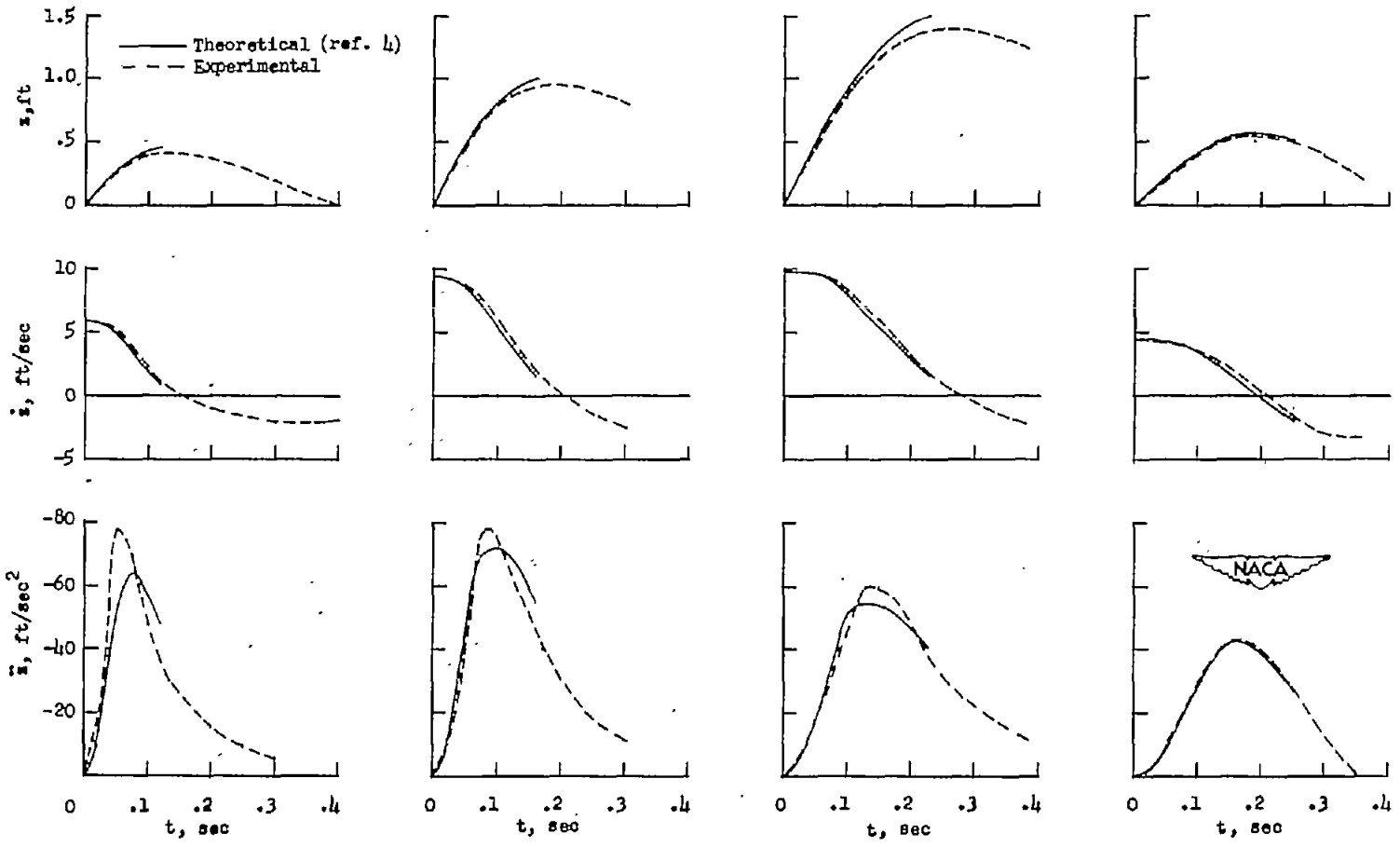

(a) Run 1. $\tau = 4^{\circ}$; $\gamma = 4.4^{\circ}$.

(b) Run 8. $\tau = 12^{\circ}$; $\gamma = 11.3^{\circ}$.

(c) Run 13. $\tau = 20^{\circ}$; $\gamma = 16.0^{\circ}$.

(d) Run 10. $\tau = 20^{\circ}$; $\gamma = 3.0^{\circ}$.

Figure 9.- Comparison of theoretical and experimental time histories of vertical motions for the V-step model.

NACA-Langley - 5-5-53 - 1000